Nonisothermal Crystallization and Melting Behavior of PP/Nanoclay/$CaCO_3$ Ternary Nanocomposite

Yasser Zare, Hamid Garmabi

Department of Polymer Engineering and Color Technology, Amirkabir University of Technology, Tehran, Iran

Received 29 April 2011; accepted 20 June 2011
DOI 10.1002/app.35134
Published online 12 October 2011 in Wiley Online Library (wileyonlinelibrary.com).

ABSTRACT: Nonisothermal crystallization and melting behavior of PP/nanoclay/$CaCO_3$ ternary nanocomposite were investigated using different melt flow index (MFI) of PP, nanoclay and $CaCO_3$ contents. The rate of crystallization was also studied using relative crystallinity as a function of temperature and time. The results show that the increase of MFI of PP and $CaCO_3$ content in the prepared ternary nanocomposite shift the crystallization curve of PP to the higher temperature. However, increasing the content of nanoclay from 2 wt % to 6 wt % decreases the crystallization temperature possibly due to the restriction of molecular chain mobility. Further analysis of nonisothermal crystallization was carried out based on Avrami equation which the crystallization kinetic of prepared nanocomposite was evaluated. Except the significant variation in the heat of melting, the influence of these parameters on the melting behavior was much less than the crystallization process. © 2011 Wiley Periodicals, Inc. J Appl Polym Sci 124: 1225–1233, 2012

Key words: PP/nanoclay/$CaCO_3$ ternary nanocomposite; nonisothermal crystallization; melting behavior

INTRODUCTION

In the recent years, nanocomposites have attracted intense interest in both academia and industries primarily due to their outstanding properties. The incorporation of rather low loading of nanoclay in polymer matrix, as the most commonly nanofiller utilized in polymer nanocomposites encourage striking mechanical, thermal and permeability performances.[1–3] The good dispersion of nanoclay in the matrix is found to be a major necessity in the development of desired properties. However, achieving homogeneous spreading of polar nanoclay layers in a nonpolar polymer such as PP could be a major challenge which often a compatibilizer such as maleic anhydride modified PP (PPgMA) is employed to improve the dispersion of nanoclay and obtain good adhesion between nanoclay layers and PP matrix.[4,5]

$CaCO_3$ nanoparticles also are the commonly filler used to develop the mechanical properties of the polymers due to their dramatic effect on increasing the interfacial area between filler and matrix.[6,7] The improvement of the mechanical properties through addition of nanosized $CaCO_3$ to polymer matrix have been shown to be much greater than those with microparticles.[8] $CaCO_3$ nanoparticles are treated with stearic acid or titan coupling agent to obtain uniform dispersion of $CaCO_3$ nanoparticles in polymer matrix and the more improvement of interface adhesion between nanoparticles and matrix.[9,10]

Recently, the simultaneous addition of nanoclay and $CaCO_3$ nanoparticles to PP matrix has been reported in the literature.[11–13] Two different nanoparticles affect the general performances of the prepared nanocomposite particularly mechanical properties. The incorporation of nanoclay to PP often decreases the impact strength[14–16] but the addition of $CaCO_3$ nanoparticles to PP/nanoclay improves the impact strength developing the application of nanocomposites in many areas. In addition, better tensile modulus was presented in PP/nanoclay/$CaCO_3$ ternary nanocomposite compared with the binary PP/nanoclay and PP/$CaCO_3$ nanocomposites.[13] Therefore, the PP/nanoclay/$CaCO_3$ ternary nanocomposite is valuable for investigation.

It is worth noting that uniformly dispersed nanofillers affect the crystallization and melting behavior of PP attributed to the nucleation effect of nanoparticles.[17–20] In addition, it was suggested that the interaction between polymer and nanofillers affects the crystallization rate of matrix on the filler surface introducing a new opening in investigating of the crystallization and melting behavior of nanocomposites.[21,22] In this regard, there are a number of reports in the literature on the PP/nanoclay and PP/$CaCO_3$ binary nanocomposites, but limited works exist on the application of two nanofillers. The analysis of the nonisothermal crystallization process is more difficult than isothermal due to temperature variation. However, nonisothermal crystallization provides valuable information about the nanocomposite crystalline development because the

Correspondence to: H. Garmabi (Garmabi@aut.ac.ir).

crystallization behavior has remarkable influence on the final properties of nanocomposites such as tensile modulus and impact strength[23,24]; for this reason, the crystallization analysis of prepared ternary nanocomposite is worthwhile.

In this article, the effect of MFI of PP, nanoclay and $CaCO_3$ contents on the nonisothermal crystallization and melting behavior of PP in PP/nanoclay/$CaCO_3$ ternary nanocomposite was evaluated using differential scanning calorimetry (DSC). Moreover, the influence of the considered parameters on the crystallization kinetics was also studied based on Avrami equation.

EXPERIMENTAL

Materials

Two grades of PP homopolymer were used in this study. PP4 (Turkmen Plast TNGIZT, MFI = 4 g/10 min, 230°C, 2.16 kg) was supplied from Turkmen Bashi refinery, Turkmenistan and PP16 (VCS, MFI = 16 g/10 min, 230°C, 2.16 kg) was provided from Marun Petrochemical Company, Iran. Montmorrilonite clay modified with a quaternary ammonium salt (Cloisite20A) was provided from Southern Clay Products. The received clay (montmorillonite) particles are disk-like stacks of silicate layers, 1 nm thick and varying in diameter from 100 nm to several microns. The layer spacing (*d*-spacing) also is about 2.51 nm. Maleic anhydride grafted PP, PPgMA (PB3150, MFI = 20 g/10 min, 230°C, 2.16 kg) with 0.5 wt % of Maleic anhydride was supplied by Crompton Corp. and the precipitated $CaCO_3$ (SOCAL312) was purchased from Solvay with average size of about 70 nm coated with a layer of stearic acid.

Preparation of ternary nanocomposite

First, all materials were dried at 80°C for 10 h in an oven. They were then dry-mixed. The melt compounding was carried out in a corotating twin screw extruder, Brabender TSE 20/40D (D = 20 mm, L/D = 40). The screw speed was set at 250 rpm, the temperature was controlled at 210–230°C and feeding rate was kept at 3 kg/h. The notation used here to represent the samples is: PPn/x/y, where n is MFI of PP, x is the nanoclay weight percentage and y is the $CaCO_3$ weight percentage. The weight percentage of PPgMA in all samples is equal to that of nanoclay.

DSC analysis

Nonisothermal crystallization and melting behavior were analyzed using a PerkinElmer Diamond DSC in which temperature calibration was performed using indium standard. The samples were heated from 30 to 200°C at rate of 10°C/min and kept at this temperature for 5 min to eliminate the effect of previous thermal history; they were then cooled to 30°C at a rate of 10°C/min. All runs were carried out in a nitrogen atmosphere.

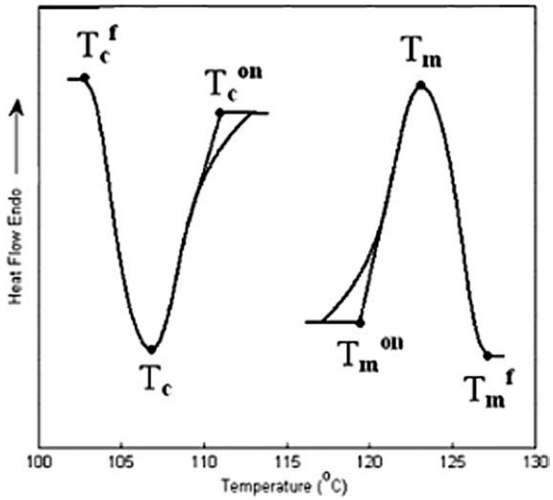

Figure 1 Schematic representation for determination of various parameters from DSC crystallization and melting peaks.

Figure 1 show a typical crystallization and melting curves in which T_c^{on} is the temperature at the onset of crystallization, T_c is the peak temperature of crystallization and T_c^f is the temperature at the crystallization completion. Also, for the melting behavior, T_m^{on} is the temperature at the onset of melting, T_m is the peak temperature of melting and T_m^f is the temperature at which the melting is completed.

The degree of crystallinity is defined according to eq. (1)[25]:

$$X_c = \frac{\Delta H_c}{w\Delta H_{100}} 100 \quad (1)$$

where ΔH_c is the crystallization heat of the sample (J/g), ΔH_{100} is the heat of crystallization for a 100% crystalline polymer, and w is the weight fraction of PP. ΔH_{100} for PP is 209 J/g.[26]

RESULTS AND DISCUSSION

Morphological observations

The nanostructure characterization of prepared samples was performed using XRD, AFM, and SEM techniques.[27,28] The observations show the mixed intercalated/exfoliated nanoclay layers as well as dispersed and distributed $CaCO_3$ nanoparticles in the PP matrix. The agglomeration and segregation of nanoparticles were not observed in all samples. The

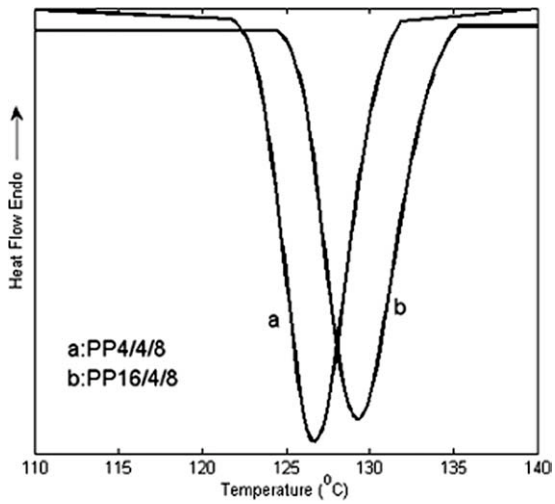

Figure 2 DSC crystallization curves of PP4/4/8 and PP16/4/8 samples.

modified nanoparticles cause more interaction and adhesion between PP chains and nanoparticles. Moreover, the high melt viscosity induced by lower MFI of PP creates high mechanical shear stress on the melt mixing that can break up the filler agglomerations well.

Effect of different MFI of PP

Figure 2 demonstrates the crystallization curves of PP4/4/8 and PP16/4/8 samples and the crystallization data are illustrated in Table I. As far as the effect of MFI of PP is concerned, it can be observed that increasing MFI of PP in ternary nanocomposite from 4 to 16 g/10 min has increased T_c^{on}, T_c, and T_c^{f}. The enhancement of crystallization temperature in the higher MFI of PP suggests that the activation of nuclei formation occur at higher temperature. The degree of crystallinity in PP16/4/8 sample is higher than PP4/4/8 sample about 3.5%. This can be due to the fact that PP with higher MFI has shorter molecular chains. There are two main effective factors in the crystallization process: one is nucleation which starts the crystallization and another is the growth of crystalline spherulites. The shorter molecular chains induce earlier and more nucleation of crystals. In addition, they have more and easier movements; therefore, more chains arrange into crystal lamellae leading to more favorable conditions for crystal growth. In addition, the dispersion level of nanoparticles in the lower MFI of PP is greater than in the higher MFI.[13,27,28] The high viscosity of melt mixing induced by the lower MFI of PP promote more shear stress to the nanoparticles facilitating the nanofiller dispersion. Clearly, the more dispersed nanoparticles involve the PP chains and limit the movement and arrangement of large PP chains into the lamella. These occurrences probably decrease the crystallinity content in the sample containing lower MFI of PP.

The relative degree of crystallinity as a function of temperature, X_T, has been defined as the ratio of exothermic peak area as follows[29]:

$$X_T = \frac{\int_{T_c^{\text{on}}}^{T} \left(\frac{dH_c}{dT}\right) dT}{\int_{T_c^{\text{on}}}^{T\infty} \left(\frac{dH_c}{dT}\right) dT} \tag{2}$$

where T_c^{on} is crystallization onset temperature and T_∞ represents the end temperature. dH_c is the enthalpy of crystallization released during an infinitesimal temperature range dT. Figure 3(a) depicts the relative crystallinity of PP4/4/8 and PP16/4/8 samples as a function of temperature. $T_{1/2}$ is defined as the half-temperature of crystallization, the temperature at which X_T is 50%. The values of $T_{1/2}$ are presented in Table II. The crystallization temperature can be transformed to the time scale to study the time parameter in the crystallization process by the following equation:

$$t = \left| \frac{T_c^{\text{on}} - T}{\varphi} \right| \tag{3}$$

where T_c^{on} is the crystallization onset temperature, T is the crystallization temperature at time (t) and φ is cooling rate. The plots of relative crystallinity as a function of time for PP4/4/8 and PP16/4/8 samples are shown in Figure 3(b).

An important parameter, the half-time of crystallization denoted by $t_{1/2}$, can be obtained from the relative crystallinity plots as a function of time. $t_{1/2}$ is defined as the change of time from the onset of crystallization to the time at which X_t is 50%. The $t_{1/2}$ values are inversely proportional to the rate of crystallization. As a result, higher $t_{1/2}$ indicates to the lower crystallization rate. The values of $t_{1/2}$ for all samples are presented in Table II. Increasing MFI of PP in ternary nanocomposite from 4 to 16 g/10 min has decreased $t_{1/2}$ from 0.49 to 0.45 min. It indicates to the enhancement of the crystallization rate with increasing MFI of PP. It could be noted that the

TABLE I
DSC Crystallization Results for All Samples

Sample	T_c^{on} (°C)	T_c (°C)	T_c^{f} (°C)	ΔH_c (j/g)	X_c (%)
PP4	122.2	116.8	112.1	91.2	43.6
PP4/4/8	132.2	127.2	123.4	84.1	45.7
PP16/4/8	133.5	129.4	125.4	90.1	49.1
PP4/2/14	134	129.3	125.7	82.6	47.1
PP4/6/14	132.2	128.1	124.1	75.1	45.1
PP4/4/20	135.1	130.4	126.8	71.5	45

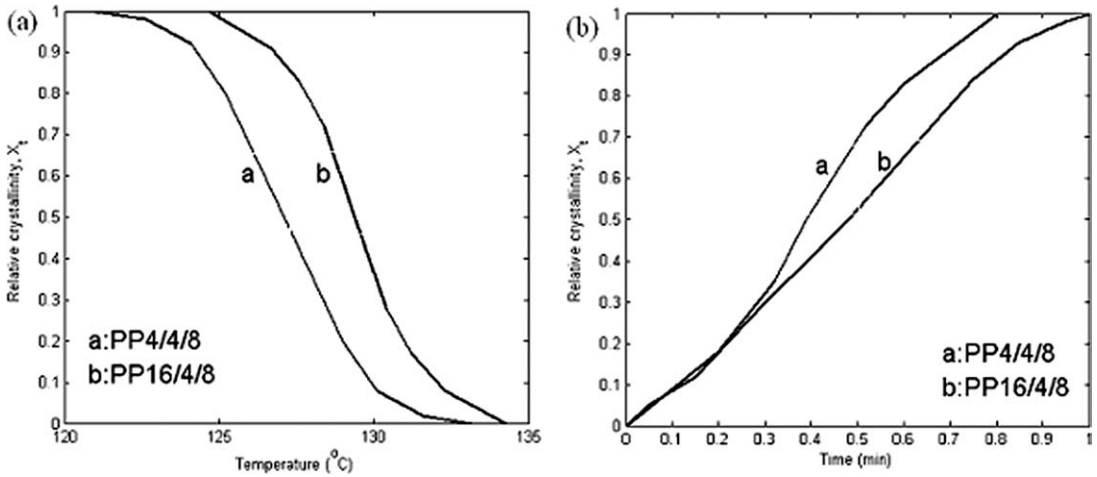

Figure 3 Development of relative crystallinity for PP4/4/8 and PP16/4/8 samples as a function of crystallization (a) temperature and (b) time.

nucleation and growth of crystals for shorter molecular chains of PP take time lower than those of larger molecular chains with lower MFI.

The crystallization kinetics of PP/nanoclay/$CaCO_3$ ternary nanocomposite has also been studied in this work. Several methods have been developed to describe the crystallization kinetics. Just like the isothermal analysis, nonisothermal crystallization can also be analyzed by the Avrami equation.[30,31] The Avrami equation is expressed as:

$$X_t = 1 - \exp(-Kt^n) \tag{4}$$

where X_t is the relative crystallinity at the crystallization time (t), n is Avrami exponent, and K is the crystallization rate constant. The Avrami equation can also be presented as eq. (5):

$$\ln[-\ln(1 - X_t)] = n\ln(t) + \ln K \tag{5}$$

According to eq. (5), the kinetic parameters, n and K can be determined from the plot of ln $[-\ln (1 - X_t)]$ versus ln (t) as the slope and the intercept of line, respectively. Figure 4 shows the same plots for PP4/4/8 and PP16/4/8 samples and the values of n and K is presented in Table II. As observed in Figure 4, the nonisothermal crystallization of prepared ternary nanocomposite follows the Avrami equation well. The value of n is 1.76 for PP4/4/8 sample which may indicate to the two dimensional growths of crystals.[32,33] Increasing MFI of PP has led to a slight variation in the value of n from 1.76 to 1.97 showing that the kinetic of crystallization does not change significantly. K is directly related to the crystallization rate and higher K value represent higher crystallization rate. The K value in the PP4/4/8 sample is lower than that in PP16/4/8 sample demonstrating the higher crystallization rate of PP16/4/8 sample. Obviously, the K results are consistent with the $t_{1/2}$ data.

Figure 5 shows the DSC melting curves of PP4/4/8 and PP16/4/8 samples and the melting data are shown in Table III.

The increment of MFI of PP from 4 to 16 g/10 min with similar nanofiller contents enhances T_m^{on},

TABLE II
Characteristic Data of the Nonisothermal Crystallization and Kinetic Parameters

Sample	$t_{1/2}$ (min)	$T_{1/2}$ (°C)	n	K (min^{-n})
PP4	0.53	117.3	2.04	0.045
PP4/4/8	0.49	127.6	1.76	0.083
PP16/4/8	0.45	129.7	1.97	0.095
PP4/2/14	0.44	131.2	2.12	0.102
PP4/6/14	0.4	128.2	1.91	0.121
PP4/4/20	0.51	130.7	2.04	0.068

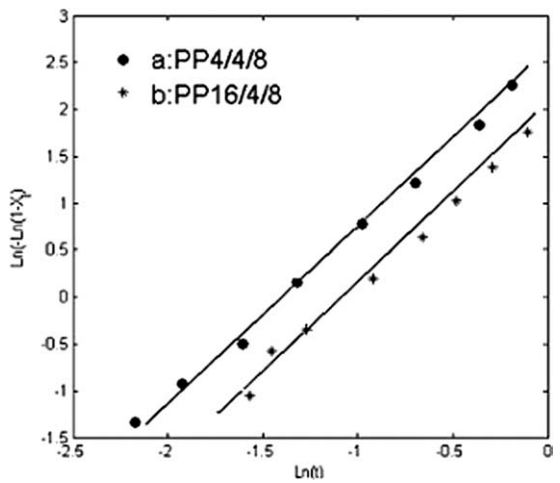

Figure 4 Plots of ln $[-\ln(1 - X_t)]$ versus ln (t) for PP4/4/8 and PP16/4/8 samples.

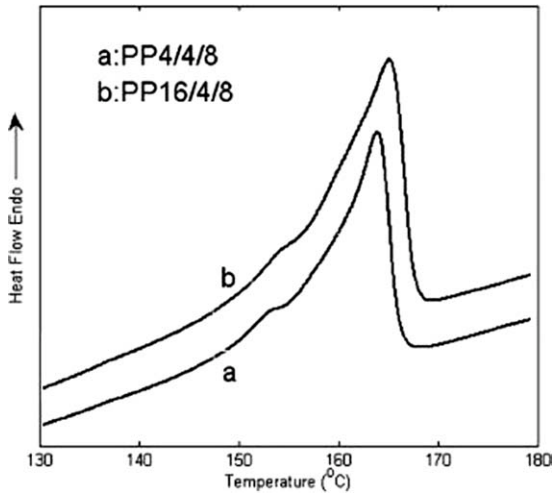

Figure 5 DSC melting curves for PP4/4/8 and PP16/4/8 samples.

T_m, and T_m^f slightly. Three phases of crystal structures namely α-, β-, and γ- can be formed in PP.[34] Among these phases, α-crystal is the most commonly and thermodynamically stable crystal structure. The formation of β-phase can be encouraged by the addition of β-nucleation particles.[35] Rodriguez et al. in their work on PP/nanoclay binary nanocomposite have shown that nanoclay in low concentration has β-nucleation effect.[36] Also, several reports have shown that surface-modified $CaCO_3$ nanoparticles in the binary nanocomposites are capable of promoting the nucleation of β-phase.[37,38]

Figure 5 shows a melting peak at about 165°C corresponding to the dominant α-crystal of PP. However, there is a small peak in the melting curve of the obtained nanocomposite at about 151°C indicating the existence of β-crystal in PP.[39] The peak intensities reveal that the amount of β-crystal is much less than α-crystal. Although nanoclay and $CaCO_3$ nanoparticles can promote the nucleation of β-crystal, it is observed in the prepared ternary nanocomposite that β-crystal is not formed as expected. This means that the β-nucleation of nanoclay and $CaCO_3$ nanoparticles are eliminated when they are added to PP simultaneously. Nanoclay is platy filler with high aspect ratio while $CaCO_3$ nanoparticles are spherical and have lower aspect ratio. In addition, nucleation sites per unit surface area in nanoclay are two orders of magnitude higher than $CaCO_3$ nanoparticles.[40] Therefore, it seems that the simultaneous addition of nanoclay and $CaCO_3$ promote more α-nucleation in PP matrix whereas the formation of β-crystal does not take place perhaps due to different specific surface area as well as the different nuclei number of the added nanofillers.

TABLE III
DSC Melting Data for All Samples

Sample	T_m^{on} (°C)	T_m (°C)	T_m^f (°C)	ΔH_m (j/g)
PP4	152.4	163	169.1	81.9
PP4/4/8	149.6	164.2	167.8	76.8
PP16/4/8	150.3	165.5	168.8	64.2
PP4/2/14	149.2	164.4	167.8	75.5
PP4/6/14	146.5	163.8	166.8	70.3
PP4/4/20	150.1	164.2	167.9	67.2

Effect of different nanoclay contents

Figure 6 shows the DSC crystallization curves of PP4, PP4/2/14, and PP4/6/14 samples to evaluate the effect of nanoclay variation at the same MFI of PP and $CaCO_3$ content. The crystallization data are presented in Table I.

The crystallization curves of PP4 and PP4/2/14 samples indicate that the addition of both 2 wt % of nanoclay and 14 wt % of $CaCO_3$ nanofillers to pure PP has caused a considerable shift in the crystallization peak toward the higher temperature by 13°C because of the heterogeneous nucleation effect of nanoparticles.

The nanoclay layers provide a large number of nucleation sites.[40] Therefore, the crystallinity degree and the crystallization temperature should be enhanced in the presence of dispersed nanoclay content.[5,36] However, contrary to this expectation, increasing nanoclay content reduced T_c, T_c^{on}, T_c^f as well as X_c. This could be attributed to the fact that the good dispersion of low loading of nanoclay creates much mechanical involvements between nanoclay layers and PP molecules. It leads to restriction of the PP molecular chain movements and consequently less crystallization of PP matrix. In addition,

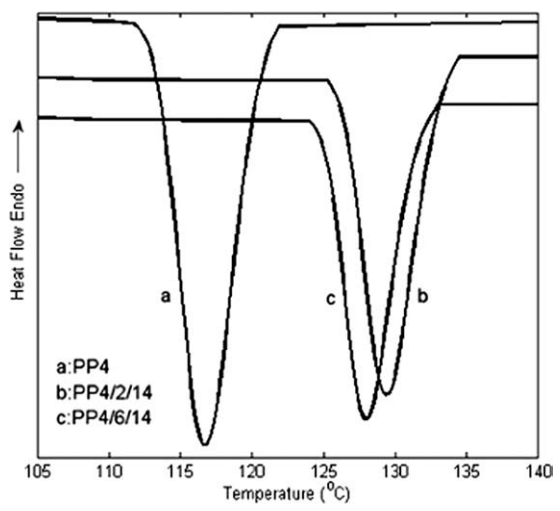

Figure 6 DSC crystallization curves of PP4, PP4/2/14 and PP4/6/14 samples.

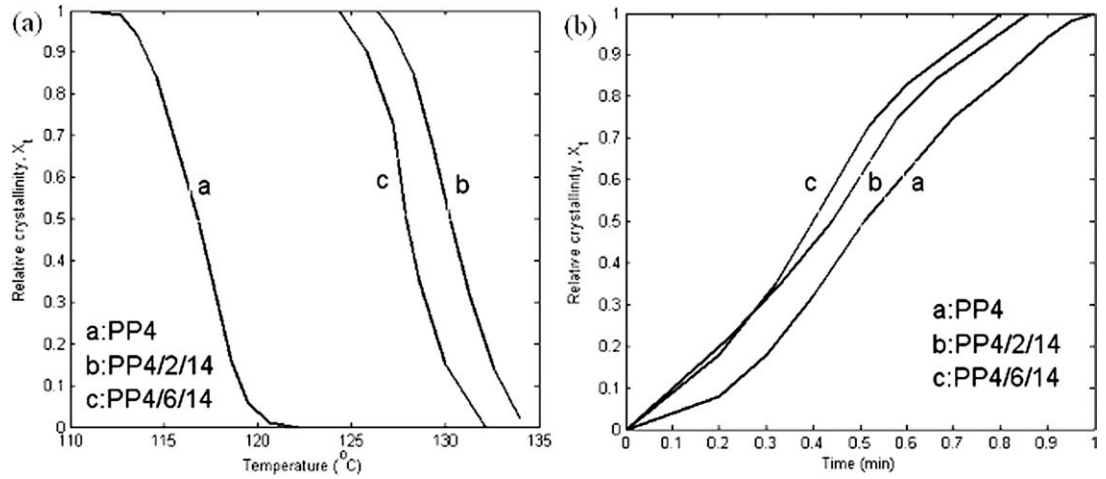

Figure 7 Development of relative crystallinity for PP4, PP4/2/14, and PP4/6/14 samples as a function of (a) temperature and (b) time of crystallization.

the presence of $CaCO_3$ nanoparticles improves the nanoclay exfoliation[13] and as a result, the movement of PP molecular chains is more decreased. Chen et al. also reported that increase in nanoclay content in the constant $CaCO_3$ content led to reduction of T_c and X_c in the PP/nanoclay/$CaCO_3$ ternary nanocomposite.[13]

The relative crystallinity as a function of temperature and time is presented in Figure 7(a,b) and the corresponding values of $T_{1/2}$ and $t_{1/2}$ are shown in Table II. The $t_{1/2}$ value in PP4/6/14 sample is slightly lower than in PP4/2/14 sample indicating the faster crystallization of PP4/6/14 sample compared with PP4/2/14 sample.

Figure 8 shows the plots of ln [−ln (1 − X_t)] versus ln (t) for PP4, PP4/2/14, and PP4/6/14 samples and the kinetic parameters, n and K are presented in Table II. The enhancement of nanoclay content decreases the n value. The value of n for PP4/2/14 sample is between 2 and 3 attributed to the instantaneous nucleation with diffusion control.[32,33] Furthermore, the value of K for PP4/6/14 sample is higher than PP4/2/14 sample showing the faster crystallization of PP4/6/14 sample.

Figure 9 shows the DSC melting curves of PP4, PP4/2/14, and PP4/6/14 samples and the melting data are presented in Table III. For the same MFI of PP and concentration of $CaCO_3$, increasing of nanoclay content has decreased T_m, T_m^f and T_m^{on} as well as ΔH_m. The reduction of T_m indicates that the enhancement of nanoclay content possibly reduced the size of lamellae and the growth of crystals as mentioned before.

As seen in Figure 9, there are hardly detectable peaks at about 151°C attributed to the formation of β-crystal of PP.[39] Further experiments are necessary

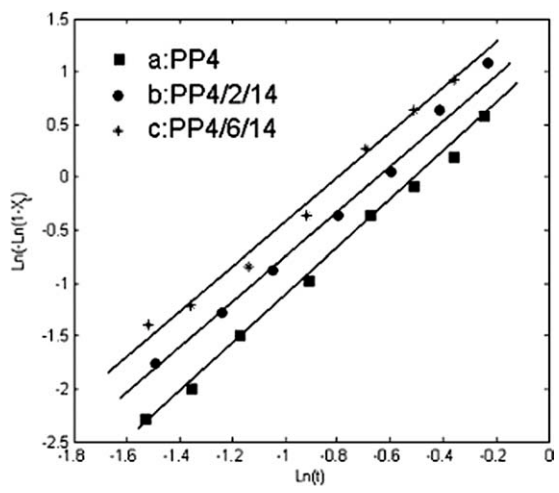

Figure 8 Plots of ln [−ln (1 − X_t)] versus ln (t) for PP4, PP4/2/14, and PP4/6/14 samples.

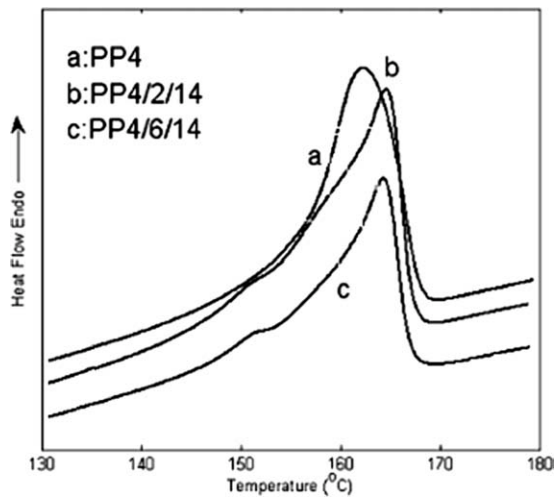

Figure 9 DSC melting curves of PP4, PP4/2/14, and PP4/6/14 samples.

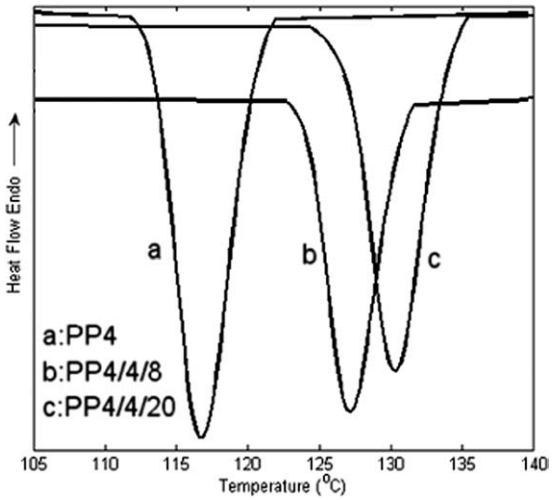

Figure 10 DSC crystallization curves of PP4, PP4/4/8, and PP4/4/20 samples.

to investigate the parameters influencing the β-nucleation effect of nanofillers when two or more nanofiller are simultaneously compounded with PP.

Effect of different $CaCO_3$ contents

Figure 10 shows the DSC crystallization curves of PP4, PP4/4/8, and PP4/4/20 samples to study the effect of $CaCO_3$ content on the nonisothermal crystallization behavior of PP/nanoclay/$CaCO_3$ ternary nanocomposite and the related data are presented in Table I.

In PP4/4/8 sample, T_c^{on}, T_c, and T_c^f are 132.2, 127.2, and 123.4°C, respectively. With increasing $CaCO_3$ content to 20 wt %, T_c^{on}, T_c, and T_c^f increase to 135.1, 130.4, and 126.8°C, respectively. This enhancement demonstrates that the $CaCO_3$ nanoparticles have strong nucleation effect activating the nuclei earlier at higher temperatures. With increasing $CaCO_3$ content, X_c decreases slightly indicating the inhibition of large crystal formation in the high concentration of $CaCO_3$ (20 wt %). The presence of $CaCO_3$ nanoparticles at about 20 wt % promotes high nucleation in the polymer matrix but the movement and arrangement of PP chains in crystalline lamellae is hindered. As mentioned in the previous section, the higher $CaCO_3$ content results in high melt viscosity. This leads to better dispersion of nanoclay layers limiting the PP molecular chain mobility more.[13,41] Therefore, lower content of crystallinity is formed in the PP4/4/20 sample compared with PP4/4/8 sample.

Figure 11(a, b) show the relative crystallinity as a function of temperature and time for PP4, PP4/4/8, and PP4/4/20 samples and the values of $T_{1/2}$ and $t_{1/2}$ are presented in Table II. The $t_{1/2}$ value in PP4/4/8 sample is lower than in PP4/4/20 sample showing the crystallization process of PP4/4/8 sample is faster. It can be probably due to the high concentration of $CaCO_3$ nanoparticles in the nanocomposite. They induce many obstacles in PP matrix preventing the diffusion of PP chains. Figure 12 shows the plots of ln [−ln (1 − X_t)] versus ln (t) for PP4, PP4/4/8, and PP4/4/20 samples and the kinetic parameters are presented in Table II. The enhancement of $CaCO_3$ content, from 8 wt % to 20 wt % changes n slightly. Also, the values of K are consistent with $t_{1/2}$ data which support the notion that the crystallization rate of PP4/4/8 sample is more than that of PP4/4/20 sample.

Figure 13 presents the DSC melting curves of PP4, PP4/4/8, and PP4/4/20 samples and the melting data are listed in Table III. The enhancement of $CaCO_3$ content does not affect T_m, T_m^f and T_m^{on}

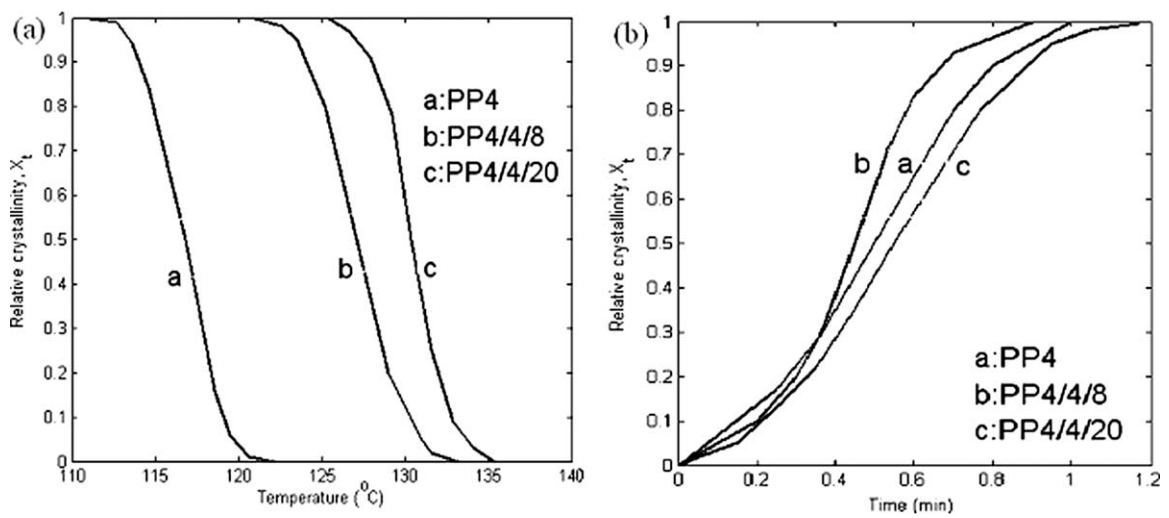

Figure 11 Development of relative crystallinity for PP4, PP4/4/8, and PP4/4/20 samples with crystallization (a) temperature and (b) time.

significantly. This suggests that the $CaCO_3$ concentration do not change the lamellar size and the growth of crystals notably. Generally, the influence of $CaCO_3$ content on the melting behavior is less significant than that of crystallization behavior. These phenomena have also been reported in PP/$CaCO_3$ binary nanocomposite where the effect of $CaCO_3$ content on the melting process was insignificant.[20] The most variation is observed in ΔH_m that with increasing $CaCO_3$ content, ΔH_m decreases due to the limitation of PP molecules by $CaCO_3$ nanoparticles.

Last, as shown in Figure 13, the enhancement of $CaCO_3$ content to 20 wt % has not change the intensity of β-phase peak more. This occurrence is due to the presence of nanoclay particles. However, more studies on the PP/nanoclay/$CaCO_3$ ternary nanocomposite are required in future to better investigation of this occurrence.

CONCLUSIONS

The effect of three parameters including MFI of PP, nanoclay and $CaCO_3$ contents on the nonisothermal crystallization and melting behavior of PP/nanoclay/$CaCO_3$ ternary nanocomposite was studied using DSC. The results indicated that increasing MFI of PP and $CaCO_3$ content caused an increase in T_c. Inversely, the increase of nanoclay content decreased T_c possibly due to the reduction of chain mobility. Although nanoparticles are expected to promote high nucleation effect in PP matrix, the crystallinity content decreased by further addition of nanoparticles. The nanoparticles in high contents seem to act as obstacles that hinder the diffusion of chains in crystal lamellae. The results obtained by Avrami equation demonstrated that the values of $t_{1/2}$ and K are consistent. Among the studied samples, the fastest crystallization process occurred for PP4/6/14 sample and the slowest one took place in PP4 sample.

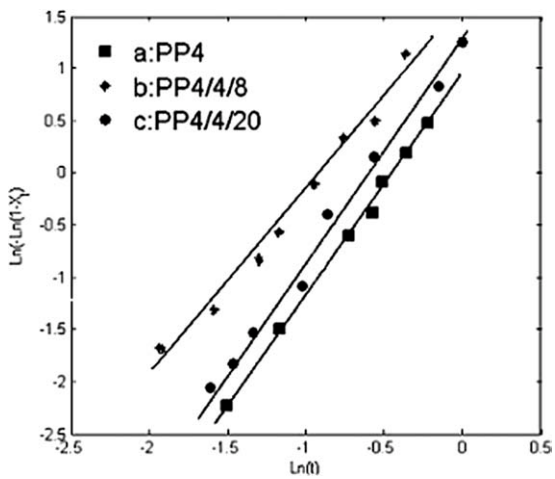

Figure 12 Plots of ln [−ln (1 − X_t)] versus ln (t) for PP4, PP4/4/8, and PP4/4/20 samples.

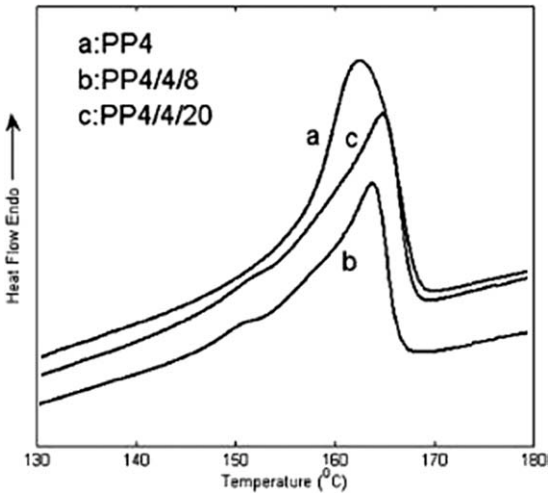

Figure 13 DSC melting curves of PP4, PP4/4/8, and PP4/4/20 samples.

The melting curves presented the hardly detectable peaks at about 151°C suggesting the formation of β-crystal of PP. It is believed that the different shape and properties of nanoparticles and interaction between two nanofillers inhibit the creation of β-phase while nanoclay and $CaCO_3$ are β-crystal nucleation in PP matrix.

References

1. Li, P.; Song, G.; Yin, L.; Wang, L.; Ma, G. J Appl Polym Sci 2008, 108, 2116.
2. Ma, J.; Qi, Z.; Hu, Y. J Appl Polym Sci 2001, 82, 3611.
3. Liu, X.; Wu, Q.; Berglund, L. A.; Lindberg, H.; Fanand, J.; Qi, Z. J Appl Polym Sci 2003, 88, 953.
4. Lee, J. W.; Kim, M. H.; Choi, W. M.; Park, O. J Appl Polym Sci 2006, 99, 1752.
5. Modesti, M.; Lorenzetti, A.; Bon, D.; Besco, S. Polymer 2005, 46, 10237.
6. Weon, J; Gam, K.; Boo, W.; Sue, H.; Chan, C. J Appl Polym Sci 2006, 99, 3070.
7. Golebiewski, J; Galeski, A. Compos Sci Technol 2007, 67, 3442.
8. Sisakht, M. R.; Khorasani, S. N.; Zadhoush, A.; Enayati, M. H.; Pezeshki, H. Polym Compos 2009, 30, 274.
9. Wang, G.; Chenl, X.; Huang, R.; Wang, L.; Chen, X. Y.; Huang, R. Mater Sci Lett 2002, 21, 985.
10. Wan, W.; Yu, D.; Xie, Y.; Guo, X.; Zhou, W.; Cao, J. J Appl Polym Sci 2006, 102, 3480.
11. Tang, Y.; Hu, Y.; Zhang, R.; Wang, Z.; Gui, Z.; Chen, Z.; Fan, W. Macromol Mater Eng 2004, 289, 191.
12. Sorrentino, L.; Berardini, F.; Capozzoli, M. R.; Amitrano, S.; Iannace1, S. J Appl Polym Sci 2009, 113, 3360.
13. Chen, H.; Wang, M.; Lin, Y.; C-Ming, C. J Appl Polym Sci 2007, 106, 3409.
14. Hasegawa, N.; Kawasumi, M.; Kato, M.; Usuki, A.; Okada, A. J Appl Polym Sci 1998, 67, 87.
15. Svoboda, P.; Zeng, C. C.; Wang, H.; Lee, J.; Tomasko, D. L. J Appl Polym Sci 2002, 85, 1562.
16. Chen, L.; Wong, S. C.; Pisharath, S. J Appl Polym Sci 2003, 88, 3298.
17. Yuan, Q.; Misra, R. D. K. Polymer 2006, 47, 4421.

18. Wang, Y.; Shen, H.; Li, G.; Mai, K. J Therm Anal Cal 2010, 99, 399.
19. Qin, J.; Chen, X.; Yu, J.; Wang, Y.; Tian, Y.; Wu, S. J Appl Polym Sci 2010, 117, 1047.
20. Zebarjad, S. M.; Tahani, M.; Sajjadi, S. Mater Process Tech 2004, 155, 1459.
21. Mitsuishi, K.; Ueno S.; Kodama, S.; Kawasaki, H. J Appl Polym Sci 2043 1991, 43.
22. Lin, Z.; Huang, Z.; Zhang, Y.; Mai, K. J Appl Polym Sci 2004, 91, 2443.
23. Jang, G. S.; Cho, W. J.; Ha, C. S.; Kim W.; Kim, H. K. Colloid Polym Sci 2002, 280, 424.
24. Yokoyama, Y.; Ricco, T. J Appl Polym Sci 1997, 66, 1007.
25. Ozawa, T. Polymer 1971, 12, 150.
26. Avalos, F.; Manchado, M., Arroyo, M. Polymer 1996, 37, 5681.
27. Zare, Y.; Garmabi, H.; Sharif, F. J Appl Polym Sci 2011, DOI: 10.1002/app.34378.
28. Zare, Y.; Garmabi, H.; Sharif, F. Preparation and Investigation of Mechanical Properties of PP/nanoclay/$CaCO_3$ Ternary Nanocomposite, MSc. Dissertation, Amirkabir University of Technology 2010.
29. Cebe, P.; Hong, S. Polymer 1986, 27, 1183.
30. Avrami, M. Chem Phys 1939, 8, 212.
31. Avrami, M. Chem Phys 1939, 9, 177.
32. Zhang, G.; Yan, D. J Appl Polym Sci 2003, 88, 2181.
33. Huang, J.-W. J Appl Polym Sci 2008, 110, 2195.
34. Karger-Kocsis, J. Polypropylene: Structure, Blends and Composites; Chapman & Hall: New York, 1995.
35. Varga, J.; Mudra, I.; Ehrenstein, G. W. J Therm Anal Cal 1999, 56, 1047.
36. M-Rodríguez, F. J.; M-Padilla, J. M.; Hsiao, B. S.; W-Mendoza, M. A.; R-Vargas, E.; S-Valdes, S. Polym Eng Sci 2007, 47, 1889.
37. Thio, Y.; Argon, A., Cohen, R.; Weinberg, M. Polymer 2002, 43, 3661.
38. Avella, M.; Cosco, S.; Lorenzo, M. L. D. Euro Polym J 2006, 42, 1548.
39. Chan, C. M.; Wu, J. S. Polymer 2002, 43, 2981.
40. McGenity, P.; Hooper, J.; Paynter, C.; Riley, A.; Nutbeem, C.; Elton, N.; Adams, J. Polymer 1992, 33, 5215.
41. Fornes, T. D.; Yoon, P. J.; Keskkula, H.; Paul, D. R. Polymer 2001, 42, 9929.